Chemiexcitation Acceleration of 1,2-Dioxetanes via a Spiro-Fused Inductive Electron-Withdrawing Motifs

Maya David[a#], Thomas Leirikh[a#], Omri Shelef[a], Sara Gutkin[a], Tal Kopp[a], Qingyang Zhou[b], Pengchen Ma[b,c], Micha Fridman[a], Kendall N. Houk[b]*, and Doron Shabat[a]*

[a]School of Chemistry, Raymond and Beverly Sackler Faculty of Exact Sciences, Tel-Aviv University, Tel Aviv 69978 Israel. [b]Department of Chemistry and Biochemistry, University of California, Los Angeles, California 90095, United States. [c]Department of Chemistry, School of Chemistry, Xi'an Key Laboratory of Sustainable Energy Material Chemistry and Engineering Research Center of Energy Storage Materials and Devices, Ministry of Education, Xi'an Jiaotong University, Xi'an 710049, China.

[#] These authors contributed equally

***Corresponding Authors:**
Doron Shabat, Email: chdoron@tauex.tau.ac.il
Kendall N. Houk, Email: houk@chem.ucla.edu

Abstract

The chemiluminescent light-emission pathway of phenoxy-1,2-dioxetane luminophores attracts growing interest within the scientific community. Dioxetane probes undergoing rapid flash-type chemiexcitation exhibit higher detection sensitivity than those with a slow glow-type chemiexcitation rate, predominantly due to the higher number of photons produced within a given time interval. We discovered that dioxetanes fused to non-strained six-member rings, with hetero atoms or inductive electron-withdrawing groups, present both accelerated chemiexcitation rates and elevated chemical stability compared to dioxetanes fused to four-member strained rings. DFT computational simulations supported the chemiexcitation acceleration observed by spiro-fused six-member rings with inductive electron-withdrawing groups of dioxetanes. Specifically, a spiro-dioxetane with a six-member sulfone ring exhibited a chemiexcitation rate 293-fold faster than that of spiro-adamantyl-dioxetane. A turn-ON dioxetane probe for the detection of the enzyme β-galactosidase, containing the six-member sulfone unit, exhibited a S/N value of 108 in LB cell growth media. This probe demonstrated a substantial increase in detection sensitivity towards *E. coli* bacterial cells expressing β-galactosidase, with an LOD value that is 44-fold more sensitive than that obtained by the adamantyl counterpart. The accelerated chemiexcitation and the elevated chemical stability presented by dioxetane containing a spiro-fused six-member ring with a sulfone inductive electron-withdrawing group, make it an ideal candidate for designing efficient turn-on chemiluminescent probes with exceptionally high detection sensitivity.

TOC Graphics

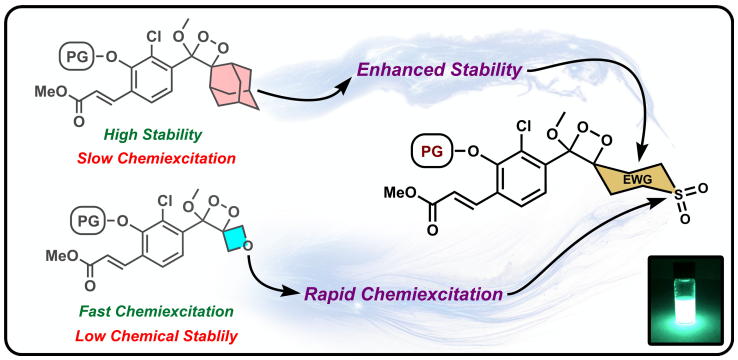

Introduction

The discovery of adamantyl-phenoxy-1,2-dioxetane chemiluminescent luminophores by the Schaap group in 1987 enabled the design of modular turn-on probes by simply masking the phenol with a triggering group, which is used as a substrate for a specific analyte of interest (Figures 1A and 1B).[1] However, the light emission generated by these dioxetanes is quenched in the presence of water, and detergent-like additives are required to enhance the light signal under physiological conditions.[2] Since these additives are highly toxic to cells, only a limited number of biocompatible applications were reported for these chemiluminescent luminophores.[3] In 2017, our group discovered that incorporating an acrylate electron-withdrawing substituent at the *ortho* position of a phenoxy-adamantyl-1,2-dioxetane chemiluminescent luminophore prevents water-mediated quenching and amplifies the light-emission intensity of the luminophore by a factor of 3000-fold (Figure 1B).[4] Noticeably, this development ended almost 30 years of dormancy in the field and enabled the use of chemiluminescent probes, for the first time, as a sole component in water with no required additives. Numerous research groups worldwide,[5-11] including ours, used the *ortho*-substituted phenoxy-adamantyl-1,2-dioxetane luminophore to develop new turn-on chemiluminescent probes for the detection and imaging of a variety of enzymes and analytes in living systems.[12-32]

Despite the encouraging progress in the field, further advancements could be attained by gaining a deeper understanding of the chemiexcitation mechanism of dioxetanes. Indeed, the chemiluminescent light-emission pathway of phenoxy-1,2-dioxetane luminophores has been capturing growing interest within the scientific community.[33-39] When the chemiexcitation rate of a given molecule is fast, light emission occurs in a flash mode. Contrariwise, if the chemiexcitation is slow, light emission takes place in a glow mode. Flash-type chemiluminescence assays generate more intense light emission signals in comparison to glow-type assays, primarily because they produce a higher number of photons within a given time interval.

The brightness of a fluorescence dye is determined by both the quantum yield and the extinction coefficient.[40] In the case of a chemiluminescence luminophore, the brightness depends on the number of photons, emitted within a specific time interval. Consequently, the luminophore's brightness is directly affected by the rate of chemiexcitation. In order to obtain a bright chemiluminophore, the compound should have both a high quantum yield and a fast chemiexcitation rate.[32] Almost a year ago, we discovered a distinct molecular motif that enables efficient enhancement of the chemiexcitation rate of dioxetane luminophores.[41] The chemiexcitation rate of phenoxy-1,2-dioxetanes was significantly accelerated through a spiro-strain-release effect, generated by a fused spiro-cyclobutane-dioxetane (Figure 1C). Remarkably, chemiluminescent 1,2-dioxetane probes, equipped with a strained cyclobutyl substituent, exhibited a diagnostic signal with a significantly high signal-to-noise ratio, resulting in unprecedented detection sensitivity toward the target enzyme.

In a structure-activity-relationship screen, we noticed that spiro-dioxetanes featuring strained four-member rings, either substituted with electron-withdrawing groups (EWGs) or with a hetero atom incorporated in the ring, exhibited higher chemiexcitation rates in comparison to their non-substituted cyclobutane counterparts.[41] However, the chemical stability of these dioxetanes was noticeably compromised due to the presence of electron-withdrawing functional groups. This observation implies that dioxetanes fused to non-strained rings, with hetero atoms or inductive electron-withdrawing groups,

may exhibit both accelerated chemiexcitation rates and elevated chemical stability (Figure 1D). We now report a substantial acceleration of the chemiexcitation rate for phenoxy 1,2-dioxetane luminophores by the incorporation of spiro-fused Inductive electron-withdrawing six-member ring motifs.

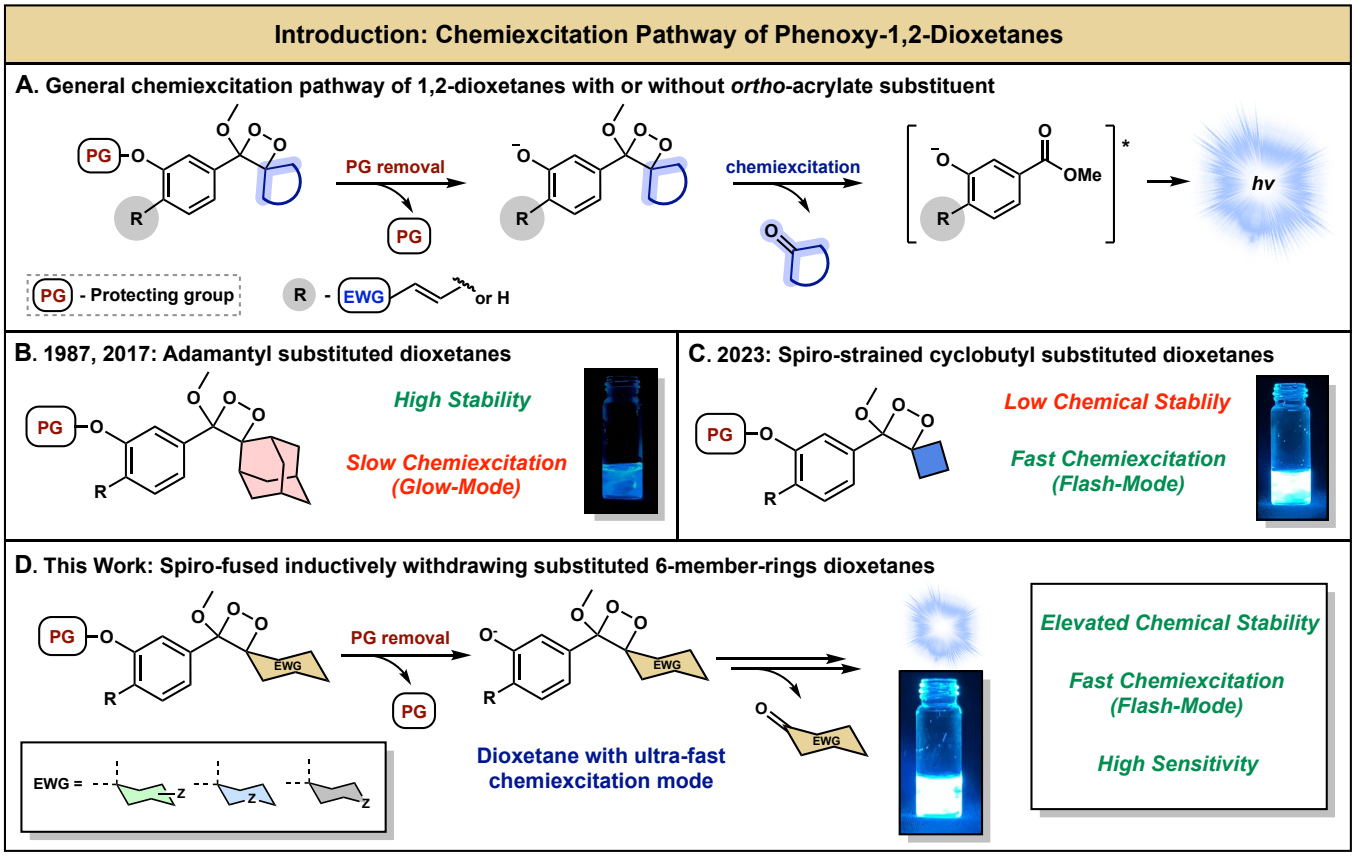

Figure 1: A. Activation and chemiexcitation pathway of 1,2-dioxetanes. B. General structure and characteristics of adamantyl substituted dioxetanes. C. General structure and characteristics of cyclobutyl substituted dioxetanes. D. This work: Electron withdrawing effect on the chemiexcitation rate.

Results and Discussion

In order to evaluate the chemiexcitation effect of a spiro-fused Inductive electron-withdrawing six-member rings, we synthesized several new phenoxy 1,2-dioxetanes, equipped with various spiro-fused six-member rings. *tert*-Butyl-dimethysilyl (TBS) triggering group was used to mask the phenols. The chemiexcitation of the dioxetanes was triggered by the removal of the TBS groups through an addition of fluoride (Figure 2A). The molecular structures of nine different spiro-cycloalkyl-dioxetanes, their stability (PBS 7.4, 37°C), total light emission half-life value ($t_{1/2}$ in DMSO or acetone), and relative chemiexcitation rates, are presented in Figure 2B. Adamantyl and cyclobutyl dioxetanes, Diox 1 and Diox 9 served as reference controls. In general, the chemiexcitation of dioxetanes is much faster in polar organic solvents like DMSO.[42] Therefore, the $t_{1/2}$ values of total light emission for dioxetanes with a relatively slow chemiexcitation rate were determined in DMSO, and for dioxetanes with a fast chemiexcitation rate measurements were conducted in acetone.

Evaluation of TBS-Masked Spiro-6-Membered-Ring Dioxetanes

A. Activation pathway of TBS-masked dioxetanes probes in the presence of TBAF

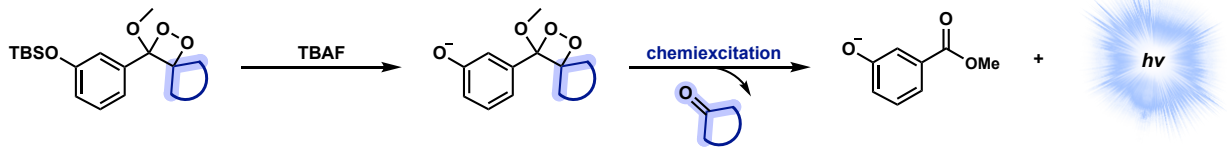

B. Chemiluminescence properties and stability of Diox 1 - Diox 9

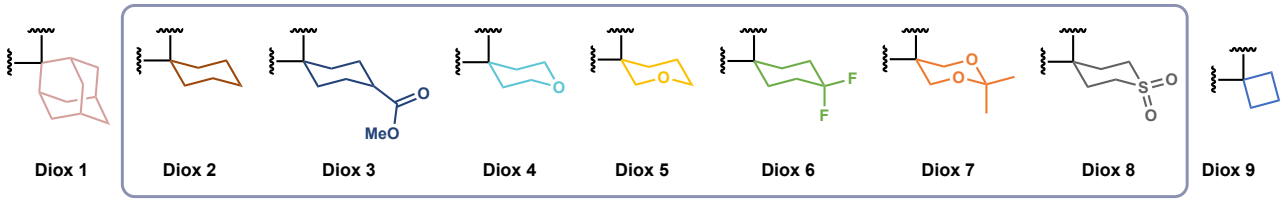

Diox 1 | Diox 2 | Diox 3 | Diox 4 | Diox 5 | Diox 6 | Diox 7 | Diox 8 | Diox 9

Probe	Stability PBS, pH 7.4 $t_{1/2}$ [h]	$t_{1/2}$ [sec] of Total Light Emission in **DMSO**	$t_{1/2}$ [sec] of Total Light Emission in **Acetone**	Relative Chemiexcitation Rate
Diox 1	**> 400**	**7.6**	**-**	**1**
Diox 2	**49.1**	**1.9**	**-**	**4.0**
Diox 3	**31.6**	**1.0**	**13.5**	**7.6**
Diox 4	**26.5**	**-**	**6.4**	**16.0**
Diox 5	**43.9**	**-**	**5.2**	**19.7**
Diox 6	**33.5**	**-**	**3.0**	**34.2**
Diox 7	**6.1**	**-**	**1.0**	**102.6**
Diox 8	**42.8**	**-**	**0.35**	**293.1**
Diox 9	**3.9**	**-**	**2.1**	**48.9**

Figure 2: A. General activation pathway of TBS-masked 1,2-dioxetanes. B. Molecular structures and chemiluminescent properties of different spiro-cycloalkyl phenoxy-1,2-dioxetanes. The stability of Diox 1-Diox 9 [500 μM] was measured in PBS, pH 7.4, 15% ACN at 37°C; product distribution was determined using RP-HPLC (70-100% or 90-100% ACN in water with 0.1% TFA). Chemiexcitation properties of Diox 1-Diox 9 [10 nM] were measured in DMSO or Acetone, with TBAF [10 mM], with 10% ACN. Half-life value ($t_{1/2}$) is defined as the time point by which half of the total light emission was observed. Relative chemiexcitation rate is defined as the ratio between the $t_{1/2}$ values of Diox 1-Diox 9. The $t_{1/2}$ of Diox 1 in DMSO was used as a reference. All measurements were conducted using SpectraMax iD3, with injector settings fixed on an integration time of 50 msec.

In agreement with our expectations, all of the phenoxy 1,2-dioxetanes with spiro-fused Inductive electron-withdrawing six-member rings, exhibited a significantly enhanced chemiexcitation rate in comparison to that of the spiro-adamantyl and cyclohexyl dioxetanes (Diox 1 and Diox 2). Remarkably, spiro-dioxetanes fused to 1,3-dioxane and sulfone electron-withdrawing motifs (Diox 7 and Diox 8) presented a chemiexcitation rate, which is 103-fold and 293-fold faster than that of the adamantyl counterpart, respectively. Intriguingly, the chemiexcitation rates of these two spiro-dioxetanes were even faster than that of the cyclobutyl-dioxetane, Diox 9 (2-fold and 6-fold respectively).

The chemical stabilities of the spiro-six-member ring dioxetanes were lower than that of the parent adamantyl derivative. This phenomenon is caused by the steric hindrance decrease in the vicinity of the dioxetane unit and the electron-withdrawing effect of the hetero atoms or polar groups presented in the six-member ring. However, all dioxetanes with spiro-fused Inductive EWG rings exhibited better chemical stabilities than the cyclobutyl derivative (Diox 9). The sulfone derivative Diox 8, exhibited both relatively high stability ($t_{1/2}$ = 42.8h) and a fast chemiexcitation rate (293-fold greater than that of Diox 1).

The chemiexcitation acceleration effect obtained by the cyclic-sulfone dioxetane Diox 8, can be clearly visualized in comparison to the chemiexcitation of the adamantyl and the cyclobutyl-dioxetanes. Figure 3 shows images of vials taken at selected time intervals for a period of 30 sec, for the chemiexcitation of the three dioxetanes in DMSO. The adamantyl-dioxetane emitted light with a relatively slow chemiexcitation rate that lasted much beyond 30 sec. The cyclobutyl-dioxetane emitted light with a significantly higher chemiexcitation rate that lasted for almost 5 sec. The 6-member cyclic-sulfone dioxetane exhibited an ultrafast chemiexcitation rate that lasted for less than a second. The relative chemiexcitation rates of the three dioxetanes were calculated by measuring their total light emission $t_{1/2}$ values according to the plots presented in Figure 3 (right). Data for processing the plots were taken from measurements obtained in Figure 2 (Figure S7-S8). Full videos of these light emission reactions are given in the supporting information.

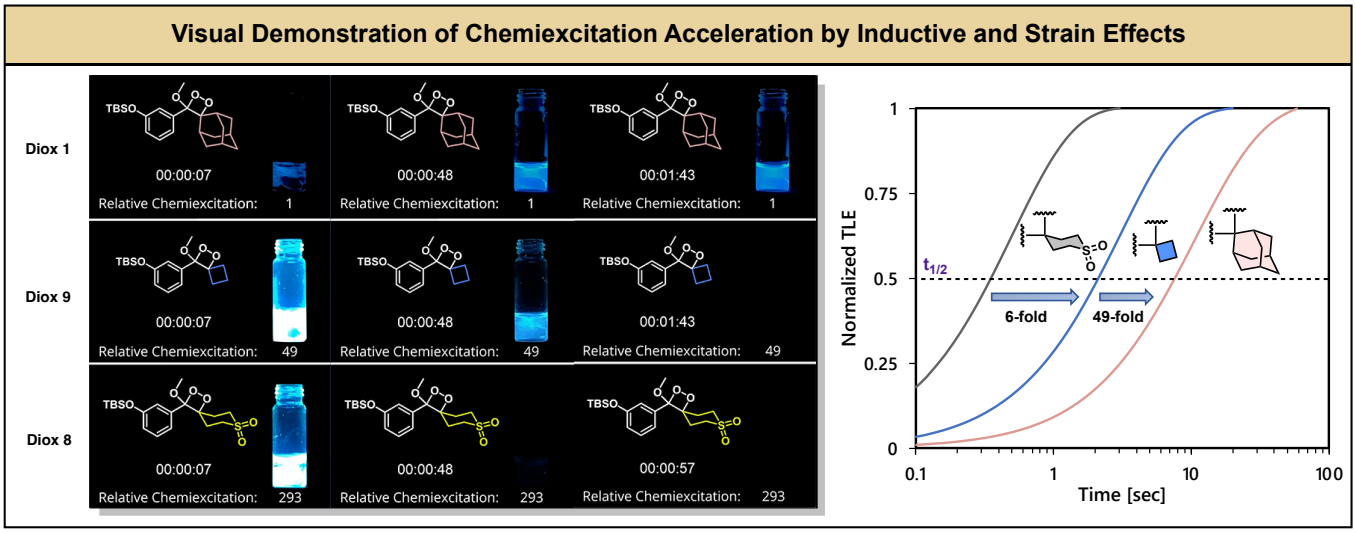

Figure 3: Visual demonstration of the light emitted by Diox 1, Diox 9, and Diox 8 [500 μM] during selected times in the presence of TBAF [20 mM] in DMSO (left). Normalized total light emission kinetic profile (time is represented in logarithmic scale) of Diox 1, Diox 9, and Diox 8 (right). The relative chemiexcitation rates are taken from Figure 2.

To better understand the chemiexcitation acceleration effect obtained by the spiro-fused inductive electron-withdrawing motifs, we conducted quantum mechanical studies with reliable DFT methods (CAM-B3LYP-D3(BJ)/6-311++G(2d,2p),SMD/ωB97XD/6-31G(d),SMD).[43, 44] It was previously shown that the mechanism of dioxetane ring opening involves charge transfer by state crossing during the O-O cleavage transition state, followed by C-C cleavage that leads in part to the luminescent excited state of the aryl ester (Figure 4A).[45] The rate-determining step of the phenoxy-1,2-dioxetane chemiexcitation involves the O-O cleavage of the dioxetane, which is accompanied by a single electron transfer (SET) from

the phenolate to the dioxetane to generate the diradical intermediate **Int1**, which can then undergo a C-C cleavage transition state **TS2_CC** to form the excited product via passing through a conical intersection (CI) point that nears **TS2_CC**.[44] The computational results of the rate-determining step (O-O cleavage transition state) for five phenoxy-1,2-dioxetanes are presented in Figure 4B.

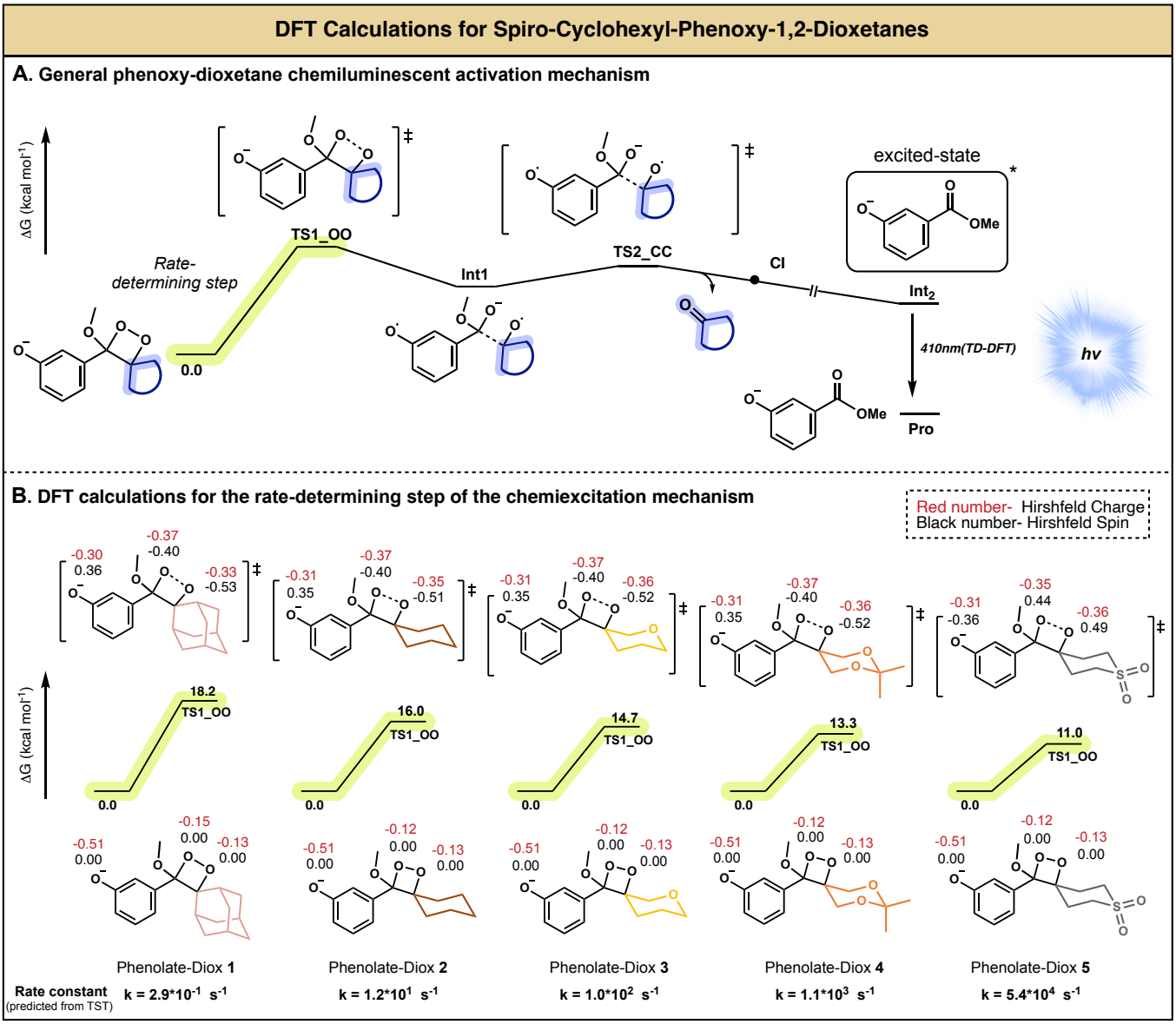

Figure 4: A. The chemiexcitation mechanism of a general spiro-cycloalkyl phenoxy-1,2-dioxetane. B. Comparison between the computed Gibbs free energy of the rate-determining step of chemiexcitation for five selected phenoxy-1,2-dioxetane. Detailed DFT calculations are presented in the supporting information (Figures S1-S5).

The adamantyl phenoxy-1,2-dioxetane (Phenolate-Diox **1**) exhibits a comparatively slow chemiexcitation rate, predicted by the relatively high barrier of 18.2 kcal/mol, for a transition state with O-O cleavage and electron transfer. Subsequently, a slightly lower barrier of 16.0 kcal/mol is predicted for the cyclohexyl phenoxy-1,2-dioxetanes (Phenolate-Diox **2**), which corresponds with a 4-fold increase in relative chemiexcitation rate observed experimentally. The introduction of electron-withdrawing substituents to the cyclohexyl ring further lowers the barrier to 14.7 kcal/mol for a single oxygen atom, 13.3 kcal/mol for

two oxygens, and 11.0 kcal/mol for sulfone. This effect can be attributed to the electronegativity of the oxygen (in Phenolate-Diox **3** and **4**) and the sulfone EWG (in Phenolate-Diox **5**), which stabilizes the anion intermediate and facilitates the electron transfer process. Figure S1-S5 shows detailed energetics, essential geometric features along the reaction path, Hirshfield charges and spin populations on important atoms involved in the reaction. Transition state theory predictions of rate constants from computed activation-free energies are also shown.

The ultrafast chemiexcitation acceleration observed for phenoxy-1,2-dioxetanes with spiro-fused six-member rings (especially for Diox 8) suggests that turn-ON probes composed of such luminophores are expected to exhibit higher detection sensitivity. To evaluate this postulate, we synthesized several new *ortho*-acrylate substituted phenoxy-1,2-dioxetanes chemiluminescent probes for the detection of β-galactosidase (β-gal) activity (Figure 5A). The probes were equipped with β-galactose as a triggering substrate and various spiro-fused six-member rings that are presented in Figure 5B. The known adamantyl and cyclobutyl-phenoxy-1,2-dioxetanes were used as control probes.
The relative chemiluminescence quantum yields of the probes were determined by measuring the total light emission produced upon activation with a high concentration of β-gal [2 U/mL] in PBS 7.4 (Figure 5B1). Interestingly, the quantum yields of all dioxetanes with fused six-member rings were up to almost 4-fold higher than that of the parent adamantyl dioxetane. The quantum yield of the cyclobutyl-dioxetane MA-Diox 9 was also 3.3-fold higher compared to the adamantyl dioxetane.

The full light emission profiles of probes MA-Diox 1, MA-Diox 2, MA-Diox 8, and MA-Diox 9 are presented in Figure 5B2. Predictably, probes MA-Diox 8 and MA-Diox 9 generate a fast light emission response with high intensity that completely decayed after 25 min. On the other hand, the light emission profile of probes MA-Diox 1 and MA-Diox 2 was significantly less intense and lasted over more than 100 min.
The light emission signals of the four selected probes were then measured under saturation kinetics conditions (low enzyme concentration). Under such conditions, the generated signal is gradually increased to a plateau level. The S/N values measured for the six-member ring sulfone and the cyclobutyl probes, MA-Diox 8 and MA-Diox 9, after 10 min (230 and 262 respectively), were substantially higher than the S/N values measured for the adamantyl and the cyclohexyl probes MA-Diox 1 and MA-Diox 2 (Figure 5B4).

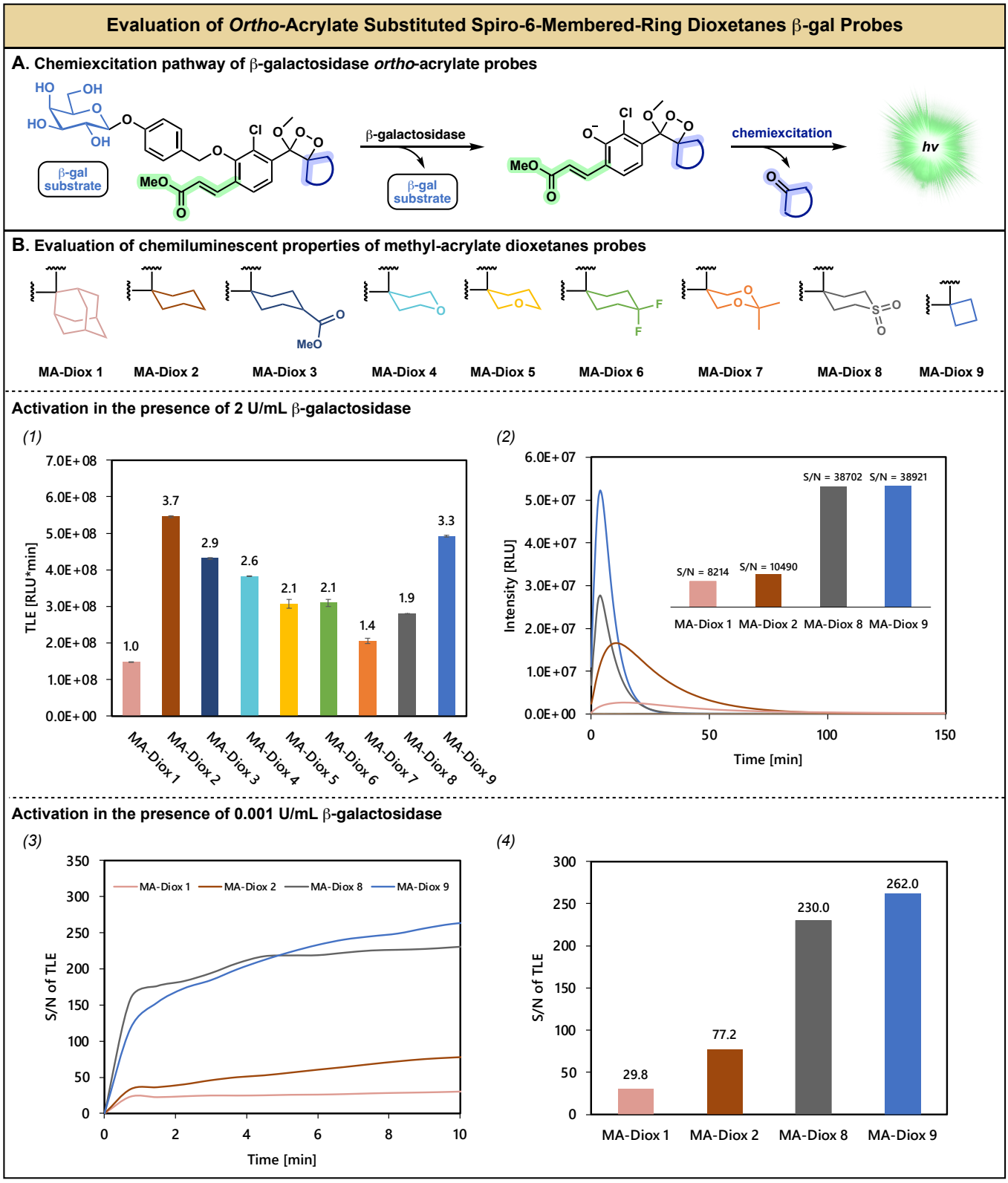

Figure 5: A. Chemiluminescent activation pathway of methyl-acrylate 1,2-dioxetanes bearing a β-galactosidase-responsive trigger. B. Molecular structures of nine analogues of methyl-acrylate 1,2-dioxetanes probes. (1) Total light emission of methyl-acrylate 1,2-dioxetanes probes [10 μM] in the presence of β-galactosidase [2 U/mL]. (2) Chemiluminescence kinetic profiles and signal-to-noise of total light emission of MA-Diox 1, MA-Diox 2, MA-Diox 8, MA-Diox 9 [10 μM] in the presence and absence of β-galactosidase [2 U/mL]. (3) Signal-to-noise of total light emission versus time of MA-Diox 1, MA-Diox 2, MA-Diox 8, MA-

Diox 9 [10 μM] in the presence and absence of β-galactosidase [0.001 U/mL]. (4) Signal-to-noise of total light emission of MA-Diox 1, MA-Diox 2, MA-Diox 8, MA-Diox 9 [10 μM] in the presence and absence of β-galactosidase [0.001 U/mL] after 10 min measurements. All measurements were conducted in PBS, pH 7.4, with 10% ACN at 27°C.

The superior chemical stability observed for sulfone Diox 8, in comparison to cyclobutyl Diox 9, indicates that probe MA-Diox 8 is a more suitable candidate for the assessment of β-gal activity in bacterial cell assays conducted in cell-growth media (Figure 6A). We next sought to evaluate the ability of the four selected probes, MA-Diox 1, MA-Diox 2, MA-Diox 8, and MA-Diox 9 to detect β-gal activity with β-gal-expressing bacterial strain *E. coli*. The stability of four probes was first measured in LB microbial growth medium.

Probes MA-Diox 1 and MA-Diox 2 exhibited high stability, with half-lives with $t_{1/2}$ of >150 h and 23.5 h respectively. Probe MA-Diox 8 demonstrated moderate stability, with $t_{1/2}$ of 3.6 hours, which is still more than satisfactory for the necessary measurements. On the other hand, the highly strained cyclobutyl probe MA-Diox 9 exhibited extremely low chemical stability in the growth medium, undergoing rapid decomposition (Figure 6B1). The lower stability of probe MA-Diox 9 in LB medium, compared to that of MA-Diox 8, is attributed to the high reactivity of the strained cyclobutyl-dioxetane toward the reducing agent's presence in the bacterial medium.

The four probes were then incubated in the presence of *Escherichia coli* ATCC 25922 in LB growth medium, and the light emission signal was monitored over 10 min. Noticeably, the S/N plot over time produced by probe MA-Diox 8 was significantly more intense than those produced by the other three probes. The S/N value obtained after 10 min with the sulfone probe MA-Diox 8 was 90-fold higher than that achieved with the adamantyl probe MA-Diox 1. As expected, the signal of the cyclobutyl probe, MA-Diox 9, owing to its high instability, resulted in a low S/N value (Figure 6B2).

Next, we sought to harness the enhanced detection sensitivity of probe MA-Diox 8 towards β-gal and its elevated chemical and thermal stability, to determine the limit of detection (LOD) for *E. coli* bacterial cells. Remarkably, The LOD value (3.9×10^4 cells) obtained by the sulfone probe MA-Diox 8 was significantly lower, indicating a 44-fold increase in sensitivity compared to that obtained by the previously known adamantyl analogue, probe MA-Diox 1 (Figure 6C). Notably, due to the moderate but sufficient chemical stability of probe MA-Diox 8, the bacterial assay could be performed directly in LB growth medium with no need for prewashing with buffer. These data clearly highlight the superior ability of probe MA-Diox 8 to detect β-gal activity in bacteria, in comparison to the other tested probes in the selected panel.

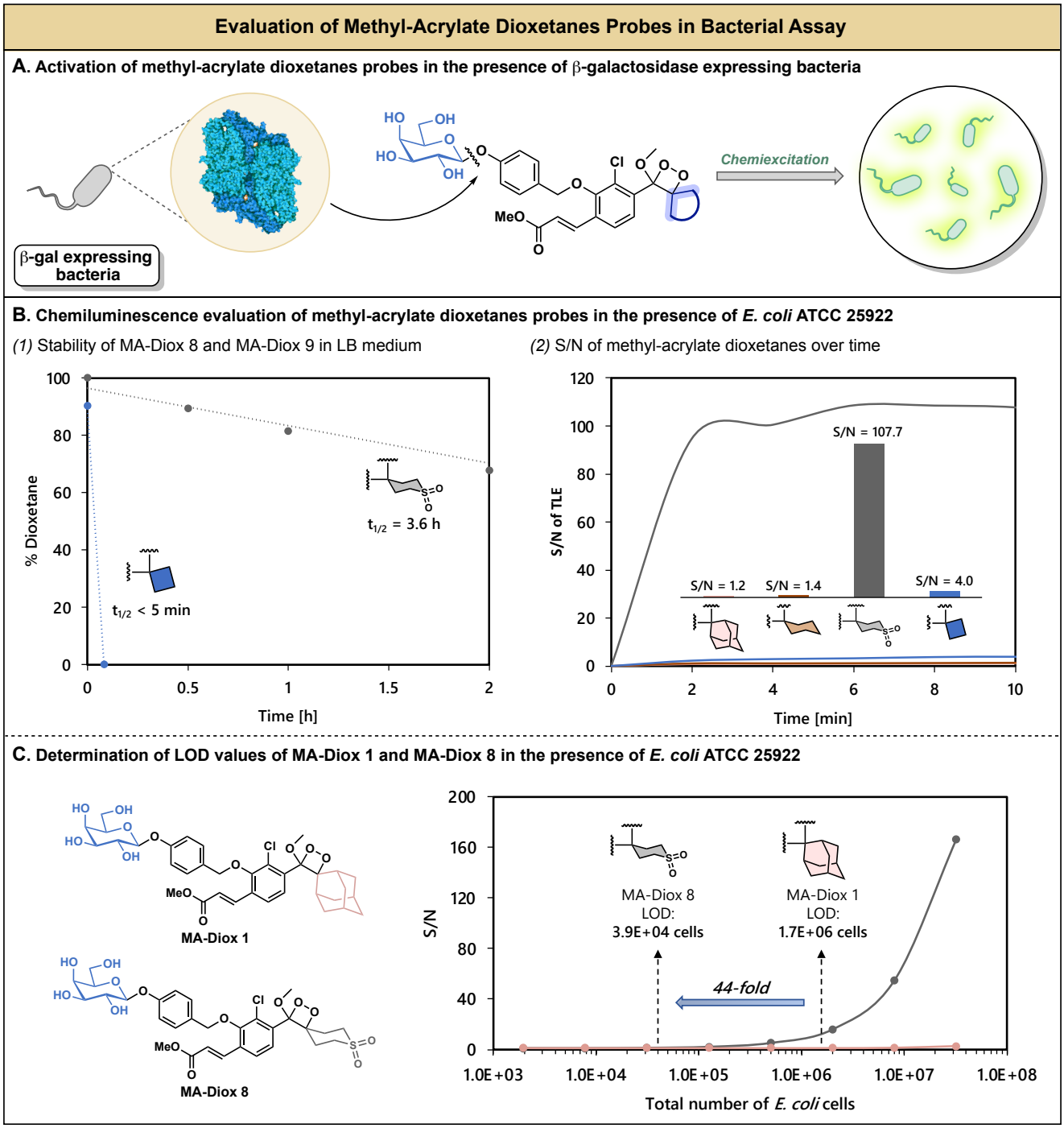

Figure 6: (A) Graphical demonstration of the activation pathway of methyl-acrylate dioxetanes probes in the presence of β-galactosidase-expressing bacteria. (B) (1) Stability of MA-Diox 8 and MA-Diox 9 [100 μM] in LB medium, 10% ACN at room temperature; product distribution was determined using RP-HPLC (30-100% ACN in water with 0.1% TFA). (2) Signal-to-noise of total light emission versus time and after 10 min measurements of MA-Diox 1, MA-Diox 2, MA-Diox 8, MA-Diox 9 [10 μM] in the presence of *E. Coli* ATCC 25922 [O.D = 0.4] in LB medium with 1% ACN at 37°C. (C) Determination of the limit of detection values of MA-Diox 1 and MA-Diox 8 [10 μM]. Measurements were taken with various concentrations of *E. coli* ATCC 25922 [1.95×10^3 to 3.20×10^7 cells), in LB medium with 1% ACN at 37°C.

As explained above, the brightness of a chemiluminescence luminophore depends on the number of photons emitted within a specific time interval. Accordingly, the luminophore's brightness increases when the rate of chemiexcitation is faster. Cyclohexyl dioxetane MA-Diox 2 has a two-fold higher chemiluminescence quantum yield compared to that of sulfone MA-Diox 8. However, its rate of chemiexcitation is substantially slower. Given these circumstances and the higher background signal observed for MA-Diox 2 versus that of MA-Diox 8, the signal-to-noise (S/N) value achieved by probe MA-Diox 8 is significantly higher than that resulting by probe MA-Diox 2 and its adamantyl analogue probe MA-Diox 1 (77-fold and 90-fold respectively, Figure 6B2).

The synthesis of the spiro-fused dioxetanes was readily achieved as described in the Supporting Information. The last step of the synthesis involves oxidation by singlet oxygen of an enolether precursor to form a dioxetane. A side ene-product of this oxidation can be obtained through the elimination of a proton positioned at the allylic position of the enolether. For a cyclobutyl-enolether, the formation of the side product is unfavored because the elimination reaction leads to the generation of a highly constrained cyclic alkene. We have previously reported that oxidation of cyclopentyl, and cycloheptyl-enolethers resulted in a full formation of the undesired ene-product.[41] The corresponding cyclohexyl derivative gave about 1:1 ratio of ene- and dioxetane products. Interestingly, oxidation of enolether attached to six-member rings with inductive electron-withdrawing properties resulted in a relatively high yield of the dioxetane product. Particularly, oxidation of the six-member ring sulfone enolether has resulted in a 91% yield of the corresponding dioxetane and only 9% of the ene-product (Figure S6).

The introduction of the spirofused-cyclobutyl-dioxetane unit as a chemiluminophore resulted in a substantial chemiexcitation acceleration effect due to the release of angular strain. Indeed, this flash chemiluminescence led to a notable enhancement in the detection sensitivity achieved by such dioxetanes, as compared to non-strained dioxetanes. Unfortunately, the chemical stability of the spiro-cyclobutyl-dioxetane was significantly compromised, and bacterial detection assays could only be performed after removing the cell growth media through prewashing with a buffer solution. Stability measurements of a spiro-cyclobutyl-dioxetane in cell-growth media resulted in the rapid decomposition of the strained dioxetane, most likely due to a reduction reaction of the peroxide bond. In this study, we observed that the inclusion of spiro-fused six-member rings with inductive electron-withdrawing properties induces a chemiexcitation acceleration effect of dioxetanes, which is comparable to the strain effect generated by the cyclobutyl units. The chemical stability of these spiro-fused six-member ring dioxetanes was notably higher and enabled their use in LB cell growth medium. The flash chemiexcitation and elevated chemical stability presented by sulfone MA-Diox 8 have resulted in a chemiluminescent probe with exceptionally high detection sensitivity and extended shelf life.

Conclusions

In summary, this study reveals a significant chemiexcitation acceleration effect of dioxetanes induced by spiro-fused six-member rings with inductive electron-withdrawing properties. Notably, spiro-dioxetanes containing six-member rings with inductive electron-withdrawing groups, exhibited substantially higher chemiexcitation rates, when compared to their spiro-adamantyl-dioxetane counterpart. The observed

acceleration effect was adequately backed up by computational calculations. Spiro-dioxetane with a 6-member sulfone ring exhibited a chemiexcitation rate that was 293-fold faster than that of spiro-adamantyl-dioxetane. A turn-ON dioxetane probe, MA-Diox 8, for the detection of β-gal activity, containing the six-member sulfone ring, exhibited a S/N value of 108 in LB cell growth medium, in the presence of *E. coli* bacterial cells. This probe demonstrated substantially increased detection sensitivity towards these bacterial cells, with an LOD value that indicates a 44-fold increase in sensitivity compared to that obtained by the previously known adamantyl analogue. The acceleration of chemiexcitation and increased chemical stability exhibited by sulfone MA-Diox 8 resulted in the development of a chemiluminescent probe with exceptionally high detection sensitivity. We expect that the chemiexcitation acceleration effect of phenoxy-1,2-dioxetane through spiro-fused six-member rings with inductive electron-withdrawing units will create new opportunities for designing innovative chemiluminescence probes with a flash mode of chemiexcitation.

References

(1) Schaap, A. P.; Chen, T. S.; Handley, R. S.; Desilva, R.; Giri, B. P. Chemical and Enzymatic Triggering of 1,2-Dioxetanes .2. Fluoride-Induced Chemiluminescence from Tert-Butyldimethylsilyloxy-Substituted Dioxetanes. *Tetrahedron Lett.* **1987**, *28*, 1155-1158.

(2) Schaap, A. P.; Akhavan, H.; Romano, L. J. Chemiluminescent substrates for alkaline phosphatase: application to ultrasensitive enzyme-linked immunoassays and DNA probes. *Clin. Chem.* **1989**, *35*, 1863-1864.

(3) Liu, L.; Mason, R. P. Imaging beta-galactosidase activity in human tumor xenografts and transgenic mice using a chemiluminescent substrate. *PLoS One* **2010**, *5*, e12024.

(4) Green, O.; Eilon, T.; Hananya, N.; Gutkin, S.; Bauer, C. R.; Shabat, D. Opening a Gateway for Chemiluminescence Cell Imaging: Distinctive Methodology for Design of Bright Chemiluminescent Dioxetane Probes. *ACS Cent. Sci.* **2017**, *3*, 349-358.

(5) Wei, X.; Huang, J. S.; Zhang, C.; Xu, C.; Pu, K. Y.; Zhang, Y. Highly Bright Near-Infrared Chemiluminescent Probes for Cancer Imaging and Laparotomy. *Angew. Chem. Int. Ed.* **2023**, *135*, e202213791.

(6) Acari, A.; Almammadov, T.; Dirak, M.; Gulsoy, G.; Kolemen, S. Real-time visualization of butyrylcholinesterase activity using a highly selective and sensitive chemiluminescent probe. *J. Mater. Chem. B* **2023**, *11*, 6881−6888.

(7) Kagalwala, H. N.; Gerberich, J.; Smith, C. J.; Mason, R. P.; Lippert, A. R. Chemiluminescent 1,2-Dioxetane Iridium Complexes for Near-Infrared Oxygen Sensing. *Angew. Chem. Int. Ed.* **2022**, *61*, e202115704.

(8) Huang, J. S.; Cheng, P. H.; Xu, C.; Liew, S. S.; He, S. S.; Zhang, Y.; Pu, K. Y. Chemiluminescent Probes with Long-Lasting High Brightness for In Vivo Imaging of Neutrophils. *Angew. Chem. Int. Ed.* **2022**, *61*, e202203235.

(9) Huang, J. S.; Jiang, Y. Y.; Li, J. C.; Huang, J. G.; Pu, K. Y. Molecular Chemiluminescent Probes with a Very Long Near-Infrared Emission Wavelength for in Vivo Imaging. *Angew. Chem. Int. Ed.* **2021**, *60*, 3999-4003.

(10) An, W. W.; Ryan, L. S.; Reeves, A. G.; Bruemmer, K. J.; Mouhaffel, L.; Gerberich, J. L.; Winters, A.; Mason, R. P.; Lippert, A. R. A Chemiluminescent Probe for HNO Quantification and Real-Time Monitoring in Living Cells. *Angew. Chem. Int. Ed.* **2019**, *58*, 1361-1365.

(11) Cao, J.; An, W. W.; Reeves, A. G.; Lippert, A. R. A chemiluminescent probe for cellular peroxynitrite using a self-immolative oxidative decarbonylation reaction. *Chem. Sci.* **2018**, *9*, 2552-2558.
(12) Shelef, O.; Kopp, T.; Tannous, R.; Arutkin, M.; Jospe-Kaufman, M.; Reuveni, S.; Shabat, D.; Fridman, M. Enzymatic Activity Profiling Using an Ultrasensitive Array of Chemiluminescent Probes for Bacterial Classification and Characterization. *J. Am. Chem. Soc.* **2024**, *146*, 5263–5273.
(13) Shelef, O.; Gutkin, S.; Feder, D.; Ben-Bassat, A.; Mandelboim, M.; Haitin, Y.; Ben-Tal, N.; Bacharach, E.; Shabat, D. Ultrasensitive chemiluminescent neuraminidase probe for rapid screening and identification of small-molecules with antiviral activity against influenza A virus in mammalian cells. *Chem. Sci.* **2022**, *13*, 12348-12357.
(14) Peukert, C.; Gholap, S. P.; Green, O.; Pinkert, L.; van den Heuvel, J.; van Ham, M.; Shabat, D.; Bronstrup, M. Enzyme-Activated, Chemiluminescent Siderophore-Dioxetane Probes Enable the Selective and Highly Sensitive Detection of Bacterial Pathogens. *Angew. Chem. Int. Ed.* **2022**, *61*, e202201423.
(15) Scott, J. I.; Gutkin, S.; Green, O.; Thompson, E. J.; Kitamura, T.; Shabat, D.; Vendrell, M. A Functional Chemiluminescent Probe for in Vivo Imaging of Natural Killer Cell Activity Against Tumours. *Angew. Chem. Int. Ed.* **2021**, *60*, 5699-5703.
(16) Gutkin, S.; Gandhesiri, S.; Brik, A.; Shabat, D. Synthesis and Evaluation of Ubiquitin-Dioxetane Conjugate as a Chemiluminescent Probe for Monitoring Deubiquitinase Activity. *Bioconjugate Chem.* **2021**, *32*, 2141-2147.
(17) Gholap, S. P.; Yao, C. Y.; Green, O.; Babjak, M.; Jakubec, P.; Malatinsky, T.; Ihssen, J.; Wick, L.; Spitz, U.; Shabat, D. Chemiluminescence Detection of Hydrogen Sulfide Release by beta-Lactamase-Catalyzed beta-Lactam Biodegradation: Unprecedented Pathway for Monitoring beta-Lactam Antibiotic Bacterial Resistance. *Bioconjugate Chem.* **2021**, *32*, 991-1000.
(18) Babin, B. M.; Fernandez-Cuervo, G.; Sheng, J.; Green, O.; Ordonez, A. A.; Turner, M. L.; Keller, L. J.; Jain, S. K.; Shabat, D.; Bogyo, M. Chemiluminescent Protease Probe for Rapid, Sensitive, and Inexpensive Detection of Live Mycobacterium tuberculosis. *ACS Cent. Sci.* **2021**, *7*, 803-814.
(19) Ye, S.; Hananya, N.; Green, O.; Chen, H. S.; Zhao, A. Q.; Shen, J. G.; Shabat, D.; Yang, D. A Highly Selective and Sensitive Chemiluminescent Probe for Real-Time Monitoring of Hydrogen Peroxide in Cells and Animals. *Angew. Chem. Int. Ed.* **2020**, *59*, 14326-14330.
(20) Yang, M. W.; Zhang, J. W.; Shabat, D. R.; Fan, J. L.; Peng, X. J. Near-Infrared Chemiluminescent Probe for Real-Time Monitoring Singlet Oxygen in Cells and Mice Model. *ACS Sens.* **2020**, *5*, 3158-3164.
(21) Gutkin, S.; Green, O.; Raviv, G.; Shabat, D.; Portnoy, O. Powerful Chemiluminescence Probe for Rapid Detection of Prostate Specific Antigen Proteolytic Activity: Forensic Identification of Human Semen. *Bioconjugate Chem.* **2020**, *31*, 2488-2493.
(22) Das, S.; Ihssen, J.; Wick, L.; Spitz, U.; Shabat, D. Chemiluminescent Carbapenem-Based Molecular Probe for Detection of Carbapenemase Activity in Live Bacteria. *Chem. Eur. J* **2020**, *26*, 3647-3652.
(23) Son, S.; Won, M.; Green, O.; Hananya, N.; Sharma, A.; Jeon, Y.; Kwak, J. H.; Sessler, J. L.; Shabat, D.; Kim, J. S. Chemiluminescent Probe for the InVitro and InVivo Imaging of Cancers Over-Expressing NQO1. *Angew. Chem. Int. Ed.* **2019**, *58*, 1739-1743.
(24) Roth-Konforti, M.; Green, O.; Hupfeld, M.; Fieseler, L.; Heinrich, N.; Ihssen, J.; Vorberg, R.; Wick, L.; Spitz, U.; Shabat, D. Ultrasensitive Detection of Salmonella and Listeria monocytogenes by Small-Molecule Chemiluminescence Probes. *Angew. Chem. Int. Ed.* **2019**, *58*, 10361-10367.

(25) Hananya, N.; Reid, J. P.; Green, O.; Sigman, M. S.; Shabat, D. Rapid chemiexcitation of phenoxy-dioxetane luminophores yields ultrasensitive chemiluminescence assays. *Chem. Sci.* **2019**, *10*, 1380-1385.
(26) Hananya, N.; Press, O.; Das, A.; Scomparin, A.; Satchi-Fainaro, R.; Sagi, I.; Shabat, D. Persistent Chemiluminescent Glow of Phenoxy-dioxetane Luminophore Enables Unique CRET-Based Detection of Proteases. *Chem. Eur. J.* **2019**, *25*, 14679-14687.
(27) Roth-Konforti, M. E.; Bauer, C. R.; Shabat, D. Unprecedented Sensitivity in a Probe for Monitoring CathepsinB: Chemiluminescence Microscopy Cell-Imaging of a Natively Expressed Enzyme. *Angew. Chem. Int. Ed.* **2017**, *56*, 15633-15638.
(28) Hananya, N.; Green, O.; Blau, R.; Satchi-Fainaro, R.; Shabat, D. A Highly Efficient Chemiluminescence Probe for the Detection of Singlet Oxygen in Living Cells. *Angew. Chem. Int. Ed.* **2017**, *56*, 11793-11796.
(29) Green, O.; Gnaim, S.; Blau, R.; Eldar-Boock, A.; Satchi-Fainaro, R.; Shabat, D. Near-Infrared Dioxetane Luminophores with Direct Chemiluminescence Emission Mode. *J. Am. Chem. Soc.* **2017**, *139*, 13243-13248.
(30) Liu, J.; Huang, J. S.; Wei, X.; Cheng, P. H.; Pu, K. Y. Near-Infrared Chemiluminescence Imaging of Chemotherapy-Induced Peripheral Neuropathy. *Adv. Mater.* **2024**, *36*, 2310605.
(31) Cheng, P. H.; Miao, Q. Q.; Li, J. C.; Huang, J. G.; Xie, C.; Pu, K. Y. Unimolecular Chemo-fluoro-luminescent Reporter for Crosstalk-Free Duplex Imaging of Hepatotoxicity. *J. Am. Chem. Soc.* **2019**, *141*, 10581-10584.
(32) Gutkin, S.; Tannous, R.; Jaber, Q.; Fridman, M.; Shabat, D. Chemiluminescent duplex analysis using phenoxy-1,2-dioxetane luminophores with color modulation. *Chem. Sci.* **2023**, *14*, 6953-6962.
(33) Blau, R.; Shelef, O.; Shabat, D.; Satchi-Fainaro, R. Chemiluminescent probes in cancer biology. *Nat. Rev. Bioeng.* **2023**, *1*, 648–664.
(34) Kagalwala, H. N.; Reeves, R. T.; Lippert, A. R. Chemiluminescent spiroadamantane-1,2-dioxetanes: Recent advances in molecular imaging and biomarker detection. *Curr. Opin. Chem. Biol.* **2022**, *68*, 102134.
(35) Haris, U.; Lippert, A. R. Exploring the Structural Space of Chemiluminescent 1,2-Dioxetanes. *ACS Sens.* **2022**, *8*, 3-11.
(36) Yang, M. W.; Huang, J. G.; Fan, J. L.; Du, J. J.; Pu, K. Y.; Peng, X. J. Chemiluminescence for bioimaging and therapeutics: recent advances and challenges. *Chem. Soc. Rev.* **2020**, *49*, 6800-6815.
(37) Hananya, N.; Shabat, D. Recent Advances and Challenges in Luminescent Imaging: Bright Outlook for Chemiluminescence of Dioxetanes in Water. *ACS Cent. Sci.* **2019**, *5*, 949-959.
(38) Gnaim, S.; Green, O.; Shabat, D. The emergence of aqueous chemiluminescence: new promising class of phenoxy 1,2-dioxetane luminophores. *Chem. Commun.* **2018**, *54*, 2073-2085.
(39) Hananya, N.; Shabat, D. A Glowing Trajectory between Bio- and Chemiluminescence: From Luciferin-Based Probes to Triggerable Dioxetanes. *Angew. Chem. Int. Ed.* **2017**, *56*, 16454-16463.
(40) Würth, C.; Grabolle, M.; Pauli, J.; Spieles, M.; Resch-Genger, U. Relative and absolute determination of fluorescence quantum yields of transparent samples. *Nat. Protoc.* **2013**, *8*, 1535-1550.
(41) Tannous, R.; Shelef, O.; Gutkin, S.; David, M.; Leirikh, T.; Ge, L.; Jaber, Q.; Zhou, Q.; Ma, P.; Fridman, M.; et al. Spirostrain-Accelerated Chemiexcitation of Dioxetanes Yields Unprecedented Detection Sensitivity in Chemiluminescence Bioassays. *ACS Cent. Sci.* **2024**, *10*, 28-42.

(42) Khalid, M.; Souza, S. P.; Cabello, M. C.; Bartoloni, F. H.; Ciscato, L. F. M. L.; Bastos, E. L.; El Seoud, O. A. A.; Baader, W. J. Solvent polarity influence on chemiexcitation efficiency of inter and intramolecular electron-transfer catalyzed chemiluminescence. *J. Photochem. Photobiol., A* **2022**, *433*, 114161.
(43) Yeh, A. H. W.; Norn, C.; Kipnis, Y.; Tischer, D.; Pellock, S. J.; Evans, D.; Ma, P.; Lee, G. R.; Zhang, J. Z.; Anishchenko, I.; et al. De novo design of luciferases using deep learning. *Nature* **2023**, *614*, 774-780.
(44) Yue, L.; Liu, Y. J. Mechanism of AMPPD Chemiluminescence in a Different Voice. *J. Chem. Theory Comput.* **2013**, *9*, 2300-2312.
(45) Tanaka, C.; Tanaka, J. Ab initio molecular orbital studies on the chemiluminescence of 1,2-dioxetanes. *J. Phys. Chem. A* **2000**, *104*, 2078-2090.